



Systematic development of a high dosage formulation to enable direct compression of a poorly flowing API: a case study

Barbara E. Schaller, Kevin M. Moroney, Bernardo Castro-Dominguez, Patrick Cronin, Jorge Belen-Girona, Patrick Ruane, Denise M. Croker, Gavin M. Walker

Publication date

01-01-2019

Published in

International Journal of Pharmaceutics;566, pp. 615-630

Licence

This work is made available under the [CC BY-NC-SA 1.0](#) licence and should only be used in accordance with that licence. For more information on the specific terms, consult the repository record for this item.

Document Version

2

Citation for this work (HarvardUL)

Schaller, B.E., Moroney, K.M., Castro-Dominguez, B., Cronin, P., Belen-Girona, J., Ruane, P., Croker, D.M. and Walker, G.M. (2019) 'Systematic development of a high dosage formulation to enable direct compression of a poorly flowing API: a case study', available: <https://hdl.handle.net/10344/8323> [accessed 24 Jul 2022].

This work was downloaded from the University of Limerick research repository.

For more information on this work, the University of Limerick research repository or to report an issue, you can contact the repository administrators at ir@ul.ie. If you feel that this work breaches copyright, please provide details and we will remove access to the work immediately while we investigate your claim.

- Supplementary Material -

Systematic development of a high dosage formulation to enable direct compression of a poorly flowing API: A case study

Barbara E. Schaller¹, Kevin M. Moroney^{1,2}, Bernardo Castro-Dominguez³, Patrick Cronin¹, Jorge Belen-Girona⁴, Patrick Ruane⁴, Denise M. Croker¹, Gavin M. Walker¹

¹*Synthesis and Solid State Pharmaceutical Centre (SSPC), Bernal Institute, University of Limerick, Limerick, Ireland.*

²*MACSI, Department of Mathematics and Statistics, University of Limerick, Limerick, Ireland.*

³*Chemical Engineering Department, University of Bath, Claverton Down, BA2 7AY Bath, United Kingdom.*

⁴*Johnson & Johnson Supply Chain, Product Supply – Manufacturing Engineering and Technology.*

Appendix / Supplementary Information

Flow characterisation

Table S1 Classification of powder flowability via Compressibility (USP29)

Compressibility Index [%]	Flow Character	Hausner Ratio
10	Excellent	1.00 – 1.11
11 – 15	Good	1.12 – 1.18
16 – 20	Fair	1.19 – 1.25
21 – 25	Passable	1.26 – 1.34
26 – 31	Poor	1.35 – 1.45
32 – 37	Very poor	1.46 – 1.59
>38	Very, very poor	>1.60

Table S2 Classification of powder flowability after Jenike.

Type of flow	Flow function value
Free-flowing	FF > 10
Easy-flowing	4 < FF < 10
Cohesive	2 < FF < 4
Very cohesive & non-flowing	FF < 2

Elastic recovery (%) of oral solid dosage forms (OSD)

The immediate axial elastic recovery percentage %ER₀ (in-die) is given by:

$$\%ER_0 = \frac{h_0 - h_p}{h_p} \times 100 \quad (S1)$$

where h_p and h_0 are the tablet thickness at maximum pressure and after the removal of the compressive force respectively. Significant elastic recovery may also occur out of die due to slower

stress relaxation. This is evaluated by measuring the axial recovery after approximately 48 hours.

This elastic recovery percentage %ER₄₈ is given by:

$$\%ER_{48} = \frac{h_{48} - h_P}{h_P} \times 100 \quad (S2)$$

where h_{48} is the tablet thickness after 48 hours. The degree of out-of-die elastic recovery can be assessed by comparing the initial response and response after 48 hours. Strong elastic recovery indicates poor inter-particle bonding and is associated with capping lamination and reduced tablet hardness and solid fraction [1, 2]. Any radial elastic recovery can be assessed in a similar manner.

Heckel analysis

Heckel analysis was performed to characterise the compressibility (pressure-porosity relationship) behaviour of blends from in-die compression data. The Heckel equation is based on the assumption that the rate of change of porosity with applied pressure P is proportional to the porosity ε . The equation is usually written in logarithmic form as:

$$\ln \frac{1}{\varepsilon} = KP + A \quad (S3)$$

where K and A are constants. The Heckel plot is a plot of $\ln \frac{1}{\varepsilon}$ against P , which typically contains a linear region at intermediate pressures. Equation (S5) is fitted to the linear region of the plot giving constants K and A . To ensure a valid comparison between materials, the compaction conditions such as punch velocity and degree of lubrication were carefully controlled. A linear fitting region of 20 – 80 MPa was chosen across all blends. The reciprocal of the slope, $1/K$, known as the mean yield pressure P_y is used to rank ease of compaction. It is related to the ability of the material to deform plastically following initial densification. Lower P_y values indicate the onset of plastic deformation at lower applied pressures. The constant A relates to the initial porosity ε_0 by

$$A = B + \ln \frac{1}{\varepsilon_0} \quad (S4)$$

where B represents the densification as a result of slippage and rearrangement of particles at low pressures.

Disintegration

The disintegration time of tablets was tested in 800 mL of deionised water at 37 °C in a disintegration apparatus (Pharma test DIST 3). Six tablets were placed into the individual sample holder tubes per basket. The disintegration time was recorded as the time taken until the last tablet was fully disintegrated following USP guidelines (USP <701>)[3]. If no disintegration took place after 15 minutes, the samples were classified as ‘not disintegrable’. The desirable disintegration time for this API was required to be less than 5 minutes.

*HPLC analysis***Table S3** HPLC information for analysis of dissolution samples

Buffer	0.75 % sodium lauryl sulphate in water at 37 °C
Testing volume	600 mL
Sampling amount	3 mL
Stirring speed:	75 rpm
Sampling intervals	5, 10, 15, 20, 30 and 45 min
HPLC conditions:	
Wavelength (UV)	225 nm
Column	Kromasil® 5C18, 250 x 4.6 mm
Column temperature	25 °C
Injection volume	10 µL
Flow rate	1 mL min ⁻¹
Mobile Phase	50/50 Acetonitrile & acidified water (pH 3)

Statistical analysis

Design of experiments (DoE) and subsequent statistical analysis was performed with the Design Expert® 9 statistical software from Stat-Ease, Inc. Further data analysis was carried out using R (version 3.4.2) with integrated development environment RStudio (version 1.1.383).

Fitting of regression models and response surfaces is performed using standard techniques. Most models in this paper are fitted using multiple linear regression. Different models are considered and model reduction is performed using analysis of variance (ANOVA) tables. Model reduction is performed by considering the p-value associated with a particular main effect, interaction or quadratic term. The p-value for each term tests the null hypothesis that the coefficient associated with a particular term is zero. A small p-value (significance level $p < 0.05$ is used here) indicates that the null hypothesis can be rejected and the term is significant in adding information to the model. Conversely, a large p-value indicates that the predictor in question cannot be used to predict changes in the response. The overall model fit is assessed using the F-test. This tests the null hypothesis that the fit of an intercept only model (constant value here) and the model in question are equal. A small p-value indicates this hypothesis can be rejected and the model has a significantly better fit than the intercept only model.

Once the significant terms have been identified, the goodness-of-fit is assessed using a combination of R-squared, adjusted R-squared, predicted R-squared measures and analysis of the residual plots. R-squared measures the percentage of the response variable variation that is explained by the fitted model. A higher R-squared value indicates a better fit to experimental data but does not account for overfitting or biased estimators. A model with too many terms may have a high R-squared but poor predictive performance due to fitting of experimental noise.

Adjusted R-squared is added to compare models with different number of terms. The R-squared increases when a new term is added, whereas adjusted R-squared increases if the new term improves the model more than would be expected by chance.

Predicted R-squared is used to consider how well the fitted model can fit new observations and is a key indicator to prevent overfitting of data. This value is calculated by removing observations from the data-set in a systematic way, estimating the new regression equation and assessing how well it can predict the removed observation. The closer the predicted R-squared is to the actual R-squared the better, while a predicted R-squared significantly lower than the R-squared value suggests there are too many terms in the model.

Analysis of the residual plots is used to check validity of the model assumptions. In order for the model to be valid, the residual errors for each observation should be normally distributed and the plot of residuals versus fitted values should show a random scatter of points above and below zero, to indicate constant variance. If these assumptions are not met the model requires further investigation.

Supplementary Material

Material database

Table S4 Material database of tested APIs, binders, disintegrant, lubricants and flow enhancer.

Material	d ₁₀ [μm]	d ₅₀ [μm]	d ₉₀ [μm]	MV [μm]	CS [m ² cc ⁻¹]	MC [%]	TD [g cm ⁻³]	CBD [g mL ⁻¹]	CP% [%]	C [kPa]	UYS [kPa]	MPS [kPa]	FF [-]	Rel _p [-]	AIF [°]	BFE [mJ]	SE [mJ g ⁻¹]	FRI [-]	SI [-]	σ _t [MPa]	ε [-]	D _T [min]
Ibuprofen	6	38	234	83	0.49	0.0	1.12	0.30	50.3	0.9	2.9	14.7	5.1	3.4	24.7	140	8.3	0.78	0.96	1.25	0.03	>15
Acetaminophen	3	24	171	59	0.79	0.1	1.29	0.34	41.9	1.7	5.9	17.8	3.0	2.4	29.9	168	8.5	1.36	0.93	0.00	0.10	0
Phenacetin	10	53	166	75	0.27	0.1	1.23	0.49	25.8	0.5	1.5	14.5	9.6	5.8	23.0	125	5.2	0.97	1.12	0.56	0.04	
Canagliflozin	8	30	62	34	0.43	0.0	1.38	0.46	28.8	0.8	3.1	17.1	5.5	4.2	33.9	188	7.7	1.19	0.79	1.77	0.44	>15
MCC PH 101	11	42	122	61	0.24	5.3	1.57	0.31	27.3	1.2	4.7	18.7	4.0	3.2	36.2	117	6.2	2.35	1.00	0.31	0.55	
MCC PH 102	85	212	322	322	0.04	4.3	1.59	0.43	17.7	0.4	1.5	17.3	11.2	8.7	36.9	197	6.1	1.74	0.98	3.78	0.18	0.5
D(+)-Lactose monohydrate	7	42	107	51	0.46	2.1	1.54	0.49	38.0	1.3	5.0	16.9	3.4	2.7	33.7	82	5.4	2.19	1.21	-	-	-
DCPD	17	56	125	67	0.18	2.9	2.53	0.80	6.5	-	-	16.8	-	-	40.3	511	6.8	1.23	1.10	1.00	0.29	>15
Kollidon CL®	23	139	224	119	0.11	3.4	1.22	0.35	11.6	0.1	0.3	15	48.8	34.5	32.6	199	6.2	1.44	1.35	0.39	0.46	0.2
Kollidon CL-F®	2	11	80	28	1.22	8.0	1.23	0.25	14.6	0.3	1.0	14.3	14.0	9.3	28.1	80	7.1	1.95	1.27	1.42	0.37	0.2
Kollidon CL-M®	1	3	8	4	2.74	5.0	1.22	0.24	28.4	0.8	2.8	15.1	5.4	4.0	31.3	29	9.0	2.98	1.67	1.13	0.34	0.5
L-HPC LH-11	18	59	159	76	0.26	-	1.48	0.35	17.6	1.7	7.8	-	5.1	-	44.0	-	-	-	-	3.44	0.23	7
L-HPC LH-21	20	56	117	65	0.17	4.1	1.46	0.45	13.9	0.3	1.3	24.6	18.5	15.5	45.0	401	9.0	1.59	0.97	2.28	0.26	12.3
L-HPC LH-31	4	19	69	33	0.76	9.4	1.47	0.33	29.2	1.6	6.8	21.7	3.2	2.7	38.9	56	8.1	4.21	1.16	3.96	0.21	>15
Metolose® 60 SH - 4000	31	73	148	84	0.11	2.2	1.28	0.44	14.0	0.3	1.3	20.5	15.4	12.4	40.4	-	-	-	-	1.63	0.16	>15
Metolose® 60 SH - 10000	30	72	155	85	0.11	3.7	1.28	0.41	15.9	0.4	1.9	23.7	12.6	10.6	45.1	399	9.8	1.88	1.14	2.09	0.17	>15
Metolose® 65 SH - 50	31	81	183	97	0.10	3.6	1.30	0.42	14.8	0.4	1.7	20.8	12.4	9.9	39.7	287	9.1	1.79	0.91	1.46	0.19	>15
Metolose® 65 SH - 400	25	67	156	81	0.12	4.2	1.31	0.37	17.4	0.2	1.1	25.4	23.4	19.9	46.8	419	11.6	1.99	1.13	2.73	0.17	>15
Metolose® 90 SH - 100 SR	26	69	165	84	0.12	4.3	1.32	0.34	17.6	0.1	0.7	29.1	41.5	36.0	49.8	422	10.5	2.05	1.02	4.38	0.13	>15
Metolose® 90 SH - 4000	27	71	176	88	0.12	6.3	1.32	0.33	19.3	0.2	0.9	27.3	31.3	26.7	47.5	346	10.1	1.82	1.09	3.75	0.15	>15
Metolose® 90 SH - SM 4000	35	100	232	120	0.09	5.5	1.34	0.23	29.4	1.3	6.0	31.1	5.2	4.4	44.6	-	-	-	-	5.47	0.10	>15
Metolose® 90 SH - 15000 SR	31	77	180	93	0.10	3.8	1.32	0.30	21.1	0.0	-	26.5	-	-	48.0	348	8.9	1.75	0.80	4.09	0.13	>15
Metolose® 90 SH - 100000 SR	27	73	196	96	0.11	4.2	1.32	0.32	21.5	0.6	3.2	28.3	8.7	7.5	47.0	322	9.4	1.88	0.97	3.96	0.13	>15
Sodium starch glycolate	-	-	-	-	-	-	1.61	0.52	11.8	0.3	1.4	21.2	15.2	12.5	42.9	328	7.0	1.64	0.92	-	-	-
Magnesium Stearate	1	6	-	-	-	3.3	1.08	0.18	40.5	0.5	1.6	13.7	8.6	5.3	23.5	18	5.5	3.33	1.47	-	-	-
Stearic acid	-	-	-	-	-	0.0	1.01	0.49	10.5	1.6	6.5	21.2	3.3	2.7	37.4	450	5.8	0.68	0.37	-	-	-
Aerosil 200	9*	23*	253*	-	-	1.4	2.88	-	-	-	-	-	-	-	-	-	-	-	-	-	-	-

*values of manufacturer

MV = mean volume diameter, CS = specific surface area, MC = moisture content, TD = true density, CBD = conditioned bulk density, CP% = compressibility percentage at 15 kPa, C = cohesion, UYS = unconfined yield strength, MPS = major principle stress, FF = flow function, Rel_p = relative flowability after Peschl, AIF = angle of internal friction, BFE = basic flow energy, SE = specific energy, FRI = flow rate index, SI = stability index, σ_t = tensile strength, ε = porosity, D_T = disintegration time

Dissolution profiles of Mixture DoE

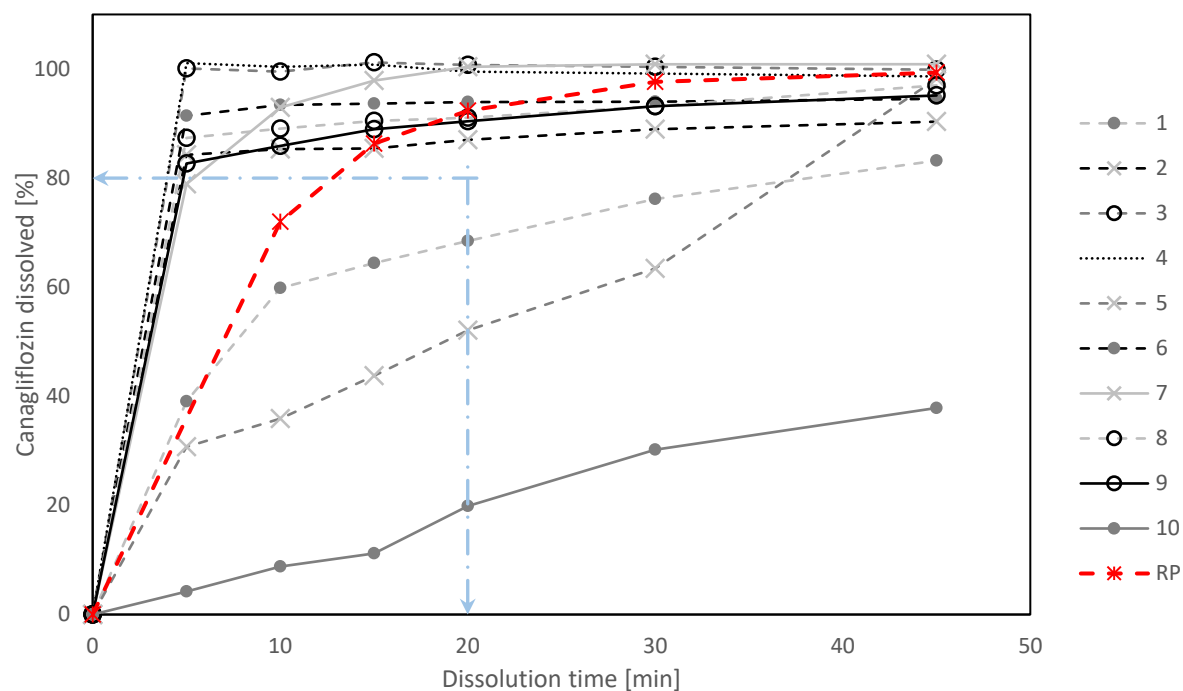


Fig. S1. Dissolution profiles of individual runs of the mixture design. The solid lines represent blends with one binder, the dashed lines indicate blends with two binders and the dotted line with three binders. The colour of the line indicates the main binder in the blend (dark grey = DCPD, black = L-HPC-LH21, light grey = MCC PH 102). The symbols indicate the smaller binder fraction in the blend (• = DCPD, o = L-HPC-LH21, x = MCC PH 102). The wet granulated commercial dissolution profile is shown in red as reference profile (RP).

Optimum amount of flow enhancer Aerosil 200

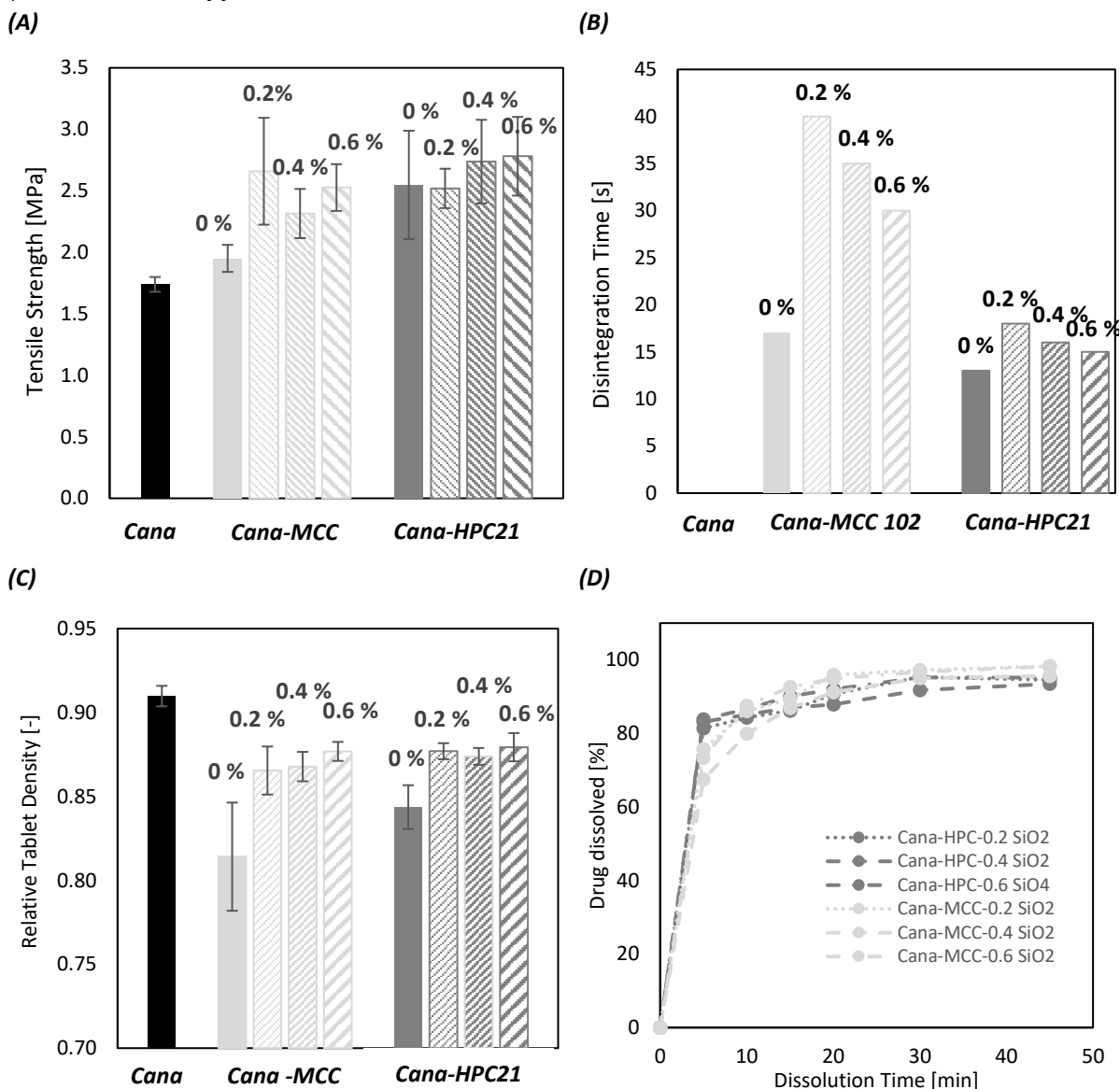


Fig. S2. Impact of silicone dioxide levels on tensile strength (A), disintegration time (B), relative density (C) and dissolution profiles (D).

References

- [1] Patel, S., Kaushal, A.M., Bansal, A.K., 2006. Compression Physics in the Formulation Development of Tablets. *Critical Reviews in Therapeutic Drug Carrier Systems* 23, 1–66. doi:10.1615/CritRevTherDrugCarrierSyst.v23.i1.10
- [2] Augsburger, L.L. and Hoag, S.W. eds., 2016. *Pharmaceutical dosage forms-tablets*. CRC Press.
- [3] United States Pharmacopeia. Chapter <701> Disintegration, USP29-NF24, 2670.